Scientific African 1 (2018) e00007

Contents lists available at ScienceDirect

Scientific African

journal homepage: www.elsevier.com/locate/sciaf

Antimicrobial photodynamic inactivation of fungal biofilm using amino functionalized mesoporus silica-rose bengal nanoconjugate against *Candida albicans*

Parasuraman Paramanantham[a], Asha P Antony[a], S.B. Sruthil Lal[b], Alok Sharan[b], Asad Syed[d], Mukhtar Ahmed[c], Abdullah A. Alarfaj[d], Siddhardha Busi[a,*], M. Maaza[e,f], K. Kaviyarasu[e,f,**]

[a] *Department of Microbiology, School of Life Sciences, Pondicherry University, Puducherry 605014, India*
[b] *Department of Physics, School of Physical, Chemical and Applied Sciences, Pondicherry University, Puducherry 605014, India*
[c] *Department of Zoology, College of Science, King Saud University, P.O. 2455, Riyadh 11451, Saudi Arabia*
[d] *Botany and Microbiology Department, College of Science, King Saud University, P.O. 2455, Riyadh 11451, Saudi Arabia*
[e] *UNESCO-UNISA Africa Chair in Nanoscience's/Nanotechnology Laboratories, College of Graduate Studies, University of South Africa (UNISA), Muckleneuk Ridge, P O Box 392, Pretoria, South Africa*
[f] *Nanosciences African Network (NANOAFNET), Materials Research Group (MRG), iThemba LABS-National Research Foundation (NRF), 1 Old Faure Road, 7129, P O Box 722, Somerset West, Western Cape Province, South Africa*

ARTICLE INFO

Article history:
Received 6 July 2018
Revised 13 September 2018
Accepted 20 September 2018

Keywords:
Antimicrobial photodynamic therapy
Mesoporus silica nanoparticles
Amino functionalization
Conjugation
Lipid peroxidation
Anti-biofilm activity

ABSTRACT

Candida albicans is an opportunistic fungal pathogen that causes both superficial and systemic infection and an important candidate that contribute to high morbidity and mortality rates in immunocompromised patients. The ability of *C. albicans* to switch from yeast to filamentous form and thereby forming biofilms make them resistant to most of the antifungal drugs available today. Thus the development of more effective antifungal drugs are essential and crucial at this point of time. Antimicrobial photodynamic therapy is an alternative modality to treat such biofilm forming resistant strains. This study aims to investigate the enhanced efficiency of newly synthesized MSN-RB conjugate as an antimicrobial photosensitizer for antimicrobial photodynamic therapy against *C. albicans*. Functionalization of MSN with amino groups was performed to increase the dye loading capacity. Conjugation process of MSN-RB was confirmed using different techniques including UV–Vis spectroscopy, Fluorescent spectroscopy and FTIR analysis. A low power green laser 50 mW irradiation was applied (5 min) for activation of MSN-RB conjugate and RB against *C. albicans* biofilm and planktonic cell. The comparative study of MSN-RB conjugate and free RB on aPDT was evaluated using standard experimental procedures. Antibiofilm efficacy was determined using biofilm inhibition assay, cell viability, EPS quantification and CLSM studies. The results revealed that MSN-RB conjugate has a significant antimicrobial activity ($88.62 \pm 3.4\%$) and antibiofilm effect on *C. albicans* when compared to free dye after light irradiation. The MSN-RB conjugate based aPDT can be employed effectively in treatment of *C. albicans* infections.

© 2018 The Authors. Published by Elsevier B.V. on behalf of African Institute of Mathematical Sciences / Next Einstein Initiative.
This is an open access article under the CC BY license.
(http://creativecommons.org/licenses/by/4.0/)

https://doi.org/10.1016/j.sciaf.2018.e00007
2468-2276/© 2018 The Authors. Published by Elsevier B.V. on behalf of African Institute of Mathematical Sciences / Next Einstein Initiative. This is an open access article under the CC BY license. (http://creativecommons.org/licenses/by/4.0/)

Introduction

The incidence of fungal infections has increased considerably and the management of these infections has become a challenge due to the incidence of resistance that can develop during therapy especially in case with use of invasive procedures, immunosuppressive medications, and broad-spectrum antibiotics, increased use of antitumor agents, HIV infections, transplant recipients and patients undergoing cancer chemotherapy etc [1]. Among them, Invasive fungal infections (IFIs) possess a major threat with high morbidity and mortality rates of about 1.5–2 million deaths every year. The increase incidence of these infections has a direct relation with increase in number of immunocompromised patients. The members of genera *Candida, Aspergillus* and *Cryptococcus* are the major candidates that cause more than 90% of life threatening invasive fungal infections. The most notorious being *Candida albicans* ranked fourth place in causing nosocomial bloodstream infections in modern hospitals with approximately 40% mortality [2]. The ability of *C. albicans* to switch from yeast to hyphal stages and biofilm formation with complex bilayer structure make them resistant to most of the antifungal agents currently available, including amphotericin B and fluconazole and appear to have multiple resistant mechanisms [3]. It is one among the ten frequent microorganisms isolated from patients with bloodstream infections and the ranked fourth in causing nosocomial bloodstream infections with 40% mortality rate. Thus the development of more effective antifungal drugs are essential and crucial at this point of time [4]. Conventional antifungal treatments with polyenes, azoles and recently launched echinocandins etc., have several limitations such as narrow therapeutic index, poor bio-availability, severe side effects and the chance of emergence of resistant strains etc. Therefore, to overcome such limitations the necessity of exploring new therapeutic strategies especially against biofilm forming and drug resistant strains are important and of top priority [5].

It is critical to note that the fungal biofilm resistance is multifactorial and this makes it difficult to develope new therapeutics targets just one of the multiple mechanisms [6]. WHO declared in 2011 that for combat drug resistance, there is no action today and no cure tomorrow. The emerging antibiotics are more potent, but they exalt the risk of systemic toxicity. So, the urgent need for an alternative strategy is essential for the survival [7]. The clear majority of research on antimicrobial resistance focuses on classical mechanisms of drug resistance against individual microbial cells in planktonic mode of life such as inactivation or modification of drug targets, bypassing the drug target, use of membrane barriers and active efflux of drugs out of the cell with the help of transporters etc. Community level resistance adds upon the cellular level resistance and this will overwhelm the effect of antibiotics. The extraordinary structure and components of biofilm, starvation-induced stringent (SOS) response, emergence of persister cells are more prevalent in biofilms and hence is a great advantage for the microorganism to rescue themselves and being resistant from higher doses of antibiotics [8,9].

According to NIH, it is estimated that about 80% of human infections are associated with biofilm forming microorganisms. Novel strategies to inhibit biofilm development and to treat biofilm associated microbial infections are currently in development. Some of the approaches aimed to alter the adhesive surfaces by physical, chemical and topographical features. Some of the approaches are meant to disturb the already established biofilms such as degradation of biofilm matrix, physical treatment of biofilms, detachment induction, introduction of signal blockers, photodynamic treatment of biofilms, novel cell-killing strategies and interference with biofilm regulation [8,10]. Antimicrobial photodynamic therapy (*aPDT*) is the best suitable, versatile, efficient and more potent treatment among all the other alternatives mentioned previously. The antimicrobial photodynamic therapy is based on the "*photodynamic effect*" which has a very unspecific mechanism of action against the microbes since the cellular damage is engender by the oxidative burst upon illumination of light to a photosensitizer so that photoresistant cells will not be generated by repeated use [11]. The three major components of *aPDT* are a nontoxic photoactive dye or a photosensitizer (PS), light of a particular wavelength - to excite the photosensitizer, molecular oxygen and other electron donors and acceptors to produce singlet oxygen and reactive oxygen species [12]. The absorption of light of a suitable wavelength converts the ground state PS to an excited singlet state. Singlet state is very unstable having its lifetime in nanosecond range and it will come to its ground state by emitting a photon through a process called fluorescence or by losing its energy as heat by internal conversion.

Otherwise, the singlet state molecule may get converted to a stable excited triplet state having its lifetime in a range of few microseconds to milliseconds via intersystem crossing that involves a spin change to an electron. Excited triplet state molecules can come back to its ground by emitting light (phosphorescence) or may react further with surrounding oxygen to produce reactive oxygen species through any of the two mechanisms designated as Type I or Type II [12,13]. Type I mechanism operates by transferring an electron or hydrogen atom to a substrate or to molecular oxygen generating reactive oxygen species like superoxide radicals, which is a precursor molecule for all the other oxygen radicals like peroxide radicals, free hydroxyl radicals etc. In type II mechanism, energy transfer occurs without the involvement of charge. Triplet state PS will transfer its energy to molecular oxygen which is also in its triplet state in normal condition get converted to highly reactive singlet oxygen. This is a more rapid technique which has a broad spectrum of action and highly economic [14].

* Corresponding author.
** Corresponding author at: UNESCO-UNISA Africa Chair in Nanoscience's/Nanotechnology Laboratories, College of Graduate Studies, University of South Africa (UNISA), Muckleneuk Ridge, P O Box 392, Pretoria, South Africa.
E-mail addresses: siddhardha.busi@gmail.com (S. Busi), kavi@tlabs.ac.za (K. Kaviyarasu).

Photosensitizers (PS) therefore play a very important role in *aPDT*. Some of the examples for PS used for *aPDT* are porphyrins, bacteriochlorins, fullerenes [15], phenothiazines, phthalocyanines, dyes such as methylene blue, rose Bengal, toluidine blue, malachite green etc [16]. Rose Bengal (RB) is a widely known anionic dye with photodynamic properties at a range of 520–540 nm wavelength was chosen for the present study. RB has been reported as a very efficient dye against yeast and also towards both gram positive and gram negative bacteria [17–19]. The combination of material science and nanotechnology improved the nanomaterials application in the field of medicine such as diagnosis of diseases, drug discovery and to treat the dreadful diseases as well as eliminating antibiotic resistant strains.

Such an approach is adopted in the present study by conjugating PS with functionalized mesoporus silica nanoparticles (MSN). The most common mesoporus silica materials are M41S, MCM-41, MCM-48 and SBA-15 with pore size ranging from 2–10 nm and 2D-hexagonal and 3D-cubic structural characteristics. Mesoporus silica nanoparticles are considered as excellent carriers for drug delivery because of their unique properties such as controlled particle size, porosity, morphology, and high chemical stability, biocompatibility, high PS loading capacity and ease of surface functionalization [20]. Researchers are interested in the biomedical application of mesoporus silica nanoparticles due to their rapid internalization into plant and animal cells without causing any cytotoxicity [21].

Studies reveal the effectiveness of methylene blue-loaded targeted mesoporous silica nanoparticles (MSNs) in the photodynamic inactivation of two Gram negative bacteria, namely *Escherichia coli* and *Pseudomonas aeruginosa* [22]. In another report carbon dots for fluorescent imaging and rose bengal as photosensitizer embedded in the core/shell structured mesoporus silica nanoparticle to perform photodynamic therapy was used [23]. The present study focused on the enhanced antimicrobial and antibiofilm activity of amino mesoporus nanoparticles-rose bengal nanoconjugate against *C. albicans* by Antimicrobial photodynamic therapy (*aPDT).*

Materials and methods

Materials and chemicals

Mesoporous silica (MSN) with 0.5 µm diameter and 0.2 nm pore size, 3-Aminopropyltrimethoxysilane (APTES, 95%), Rose Bengal (RB) were purchased from Sigma-Aldrich. All other chemicals and reagents were of chemical grade and used without any further modification.

Fungal strain and culture conditions

Candida albicans MTCC 227 (Institute of Microbial Technology, Chandigarh, India) was used for the study. *C. albicans* culture was sub cultured in special YPD media containing 1% of yeast extract, 2% dextrose, 2% peptone and 3% agar [24]. The culture was incubated in an aerobic orbital shaking incubator at 130 rpm at 37 °C. Prior to each experiment the cell numbers were estimated by measuring the optical density [OD] at 600 nm and were adjusted to 0.5 McFarland Standard (10^6 colony forming units (CFU) cells/ml).

Amino functionalization of mesoporus silica nanoparticles

Functionalization of MSN was performed by adding 25 mg of MSN and 25 µl of APTES in 25 ml ethanol. The mixture was kept under magnetic stirring for 24 hrs and subsequently centrifuged at 10,000 rpm for 10 min. The pellet was washed thrice with deionised water and dried at 60 °C in hot air oven [25].

Characterization of amino functionalised MSN

The surface functionalization of mesoporus silica nanoparticles with amino groups were confirmed using Fourier transform infrared spectroscopy (FTIR). IR spectra for functional groups were recorded using a FTIR spectroscope, Thermo Nicolet Model 6700 at a range of 400–4000 cm^{-1}. In order to prevent absorption saturation by the sample, the dyes were ground with KBr and were used for analysis [25].

Preparation of amino functionalised MSN-RB conjugate

Amino functionalized MSN (25 mg) and rose bengal (5 mg) were added to 25 ml of ethanol and kept for 48 h of magnetic stirring. After continuous stirring, the complex was separated by centrifugation at 10,000 rpm for 10 min and washed thrice with distilled water. The separated complex was dried at 60 °C in hot air oven and final powder obtained was stored in dark.

Characterization of MSN-RB conjugates

UV–Vis spectroscopic analysis

UV–Vis spectroscopic analysis was performed for amino functionalised MSN, MSN-RB and RB using Varian Carry 5000 model UV-VIS-NIR spectrophotometer. The UV–Vis scan was carried out in the range of 200–800 nm at room temperature.

Fourier transform infrared (FTIR) analysis

FTIR transmission spectra were recorded for MSN and amino functionalised MSN to confirm the functionalization. Amino functionalised MSN-RB nanoconjugate and RB spectra were also analysed to understand the conjugation by using an FTIR spectroscope, Thermo Nicolet Model 6700. The powdered samples were mixed in KBr pellets and used for FTIR analysis. For all samples, the spectrum was recorded from 400–4000 cm^{-1}.

Fluorescent spectroscopic analysis

Fluorescent emission spectra and excitation spectra was carried out for RB and MSN-RB using Jobin Yvon (Model: FLUOROLOG - FL3-11) Spectroflurometer. Photoluminescence (PL) spectroscopy is an efficient, contactless, non-destructive and widely used technique for the analysis of the optoelectronic properties of materials with less sample manipulation.

HRTEM analysis

The prepared MSN-RB nanoconjugate was subjected to High Resolution Transmission Electron Microscopic analysis. The sample for HRTEM characterization was prepared by placing a drop of colloidal solution on carbon-coated copper grid and dried at room temperature. HRTEM micrograph was captured .

Dye loading capacity and entrapment efficiency of functionalised MSN

To investigate the dye loading capacity and entrapment efficiency of amino functionalised MSN, 2 mg of prepared conjugate was added to 1 ml of ethanol and centrifuged at 10,000 rpm for 10 min. After centrifugation, the concentration of RB in supernatant solution was analysed using UV–Vis spectrophotometer at 540 nm wavelength. A standard curve of RB was plotted (10–100 µg) and the amount of dye loaded was determined using the standard curve [26]. The dye loading capacity and entrapment efficiency of MSN was calculated by the following equation:

Loading capacity(%)=(weight of loaded dye/weight of dye loaded MSN) × 100%

Entrapment efficiency(%)=(weight of loaded dye/weight of dye in feed) × 100%

In vitro RB release from MSN

In vitro release study of RB from MSN was performed using UV–Vis spectrophotometric method. About 2 mg of prepared MSN-RB conjugate was added to 2 ml of acid ethanolic media (100 mM acetic acid) and incubated at 37 °C with gentle shaking at 100 rpm. At every 30 min interval, the solution was centrifuged and OD of the supernatant at 540 nm was recorded to determine the RB release. About 2 ml of acid ethanolic media was again poured to the pellet and kept in shaking condition, centrifuged and reading was taken at 540 nm. This was continued at every 30 min intervals until the supernatant became colourless [22, 42]. The periodic release of dye from functionalised MSN was calculated using the standard curve of RB. The percentage release of dye was calculated using the formula;

$$\text{Percentage of RB released} = \frac{\text{Amount of dye released (mg/ml)}}{\text{Amount of RB in MSN–RB (mg/ml)}} \times 100$$

Cellular uptake study

C. albicans culture used in the study was adjusted to 0.5 McFarland standard by measuring OD at 600 nm prior to cellular uptake study. After centrifugation the cultures were suspended in 7 ml of phosphate buffered saline (PBS) at pH 7.4. Cellular uptake study was performed separately for free dye and MSN-RB conjugate. About 21 µl of dye from 5 mg/ml stock was added in 7 ml of cultures and a final concentration of 15 µg/ml was maintained. About 3.5 mg of conjugate was added in 7 ml of cultures for the uptake study. The solution was incubated at 37 °C with gentle shaking (120 rpm) in dark. At constant time interval (every 1 h), 2 ml of culture solution was taken and centrifuged at 10,000 rpm for 5 min. The pellet obtained was washed twice with PBS and the cell bound dye was extracted by adding methanol followed by centrifugation at 13,000 rpm. The supernatant was examined at 540 nm using UV–Vis spectrophotometer and amount of RB was determined from OD value by comparing with the standard curve [27, 43]. The percentage of dye uptake was calculated by using formula:

$$\text{Dye uptake (\%)} = \frac{\text{Amount of RB in the pellet}}{\text{Total amount of RB added}} \times 100$$

Photosensitizer and light source

Amino functionalized MSN-Rose Bengal (MSN-RB) was used as a photosensitiser and the results were compared with rose bengal. A stock solution of 5 mg/ml of both MSN-RB and RB was prepared in distilled water and stored at 4 °C in the dark. A 50 mW laser wavelength 532 nm was used to irradiate both the nanoconjugate and free RB dye (the λ_{max} of RB is 540 nm). Energy fluence was calculated according to Misba et al. [32].

Energy fluence = Power density × Time

where power density (PD) is = P (mW)/Area (cm^2), P is the output power of the light source (50 mW) and A is the irradiated area (0.635 cm^2). The beam diameter was 4.5 mm and the energy fluence was set to 94.9 J cm^{-2} when irradiated for 5 min.

Antimicrobial photodynamic inactivation of planktonic cells

Antimicrobial photodynamic inactivation of planktonic cells was carried out according to the procedure followed in Hsieh et al. [11] with slight modifications. The *C. albicans* culture was centrifuged at 10,000 rpm for 10 min and the pellet obtained was washed twice using PBS buffer. The pellet was suspended in sterile PBS and the number of cells was adjusted to 0.5 McFarland standard by taking OD at 600 nm. About 250 µl of culture was transferred to four eppendorf tubes (0.5 ml). Among four eppendorfs with culture, one was treated with amino functionalised MSN (50 µg/ml), second with RB (50 µg/ml), the other with nanoconjugate (50 µg/ml) and one with culture only. After addition of compounds, the cultures were incubated for 3 h in dark.

After incubation, the eppendorfs were centrifuged at 10,000 rpm for 5 min and pellet was collected. To the pellet equal volume of PBS was added and 200 µl was dispensed to 96 well microtitre plates. Two sets of microtitre plates were prepared for dark and light treatments. After that one set was exposed to 532 nm laser such that each well is irradiated for 5 min. The other set kept as such in dark without disturbing. The irradiated and nonirradiated plates were serially diluted 10-fold and 10^{-3} and 10^{-4} dilutions were plated. The plates were incubated for 48 hrs at 37 °C and results were recorded. The numbers of colony forming units were calculated and the percentage reduction in number of cells was determined by comparing the treated samples with untreated culture (control). From the serially diluted samples, 5 µl of 10^{-4} dilution of each treated sample was carefully spotted onto YPD agar plates. Control cultures of both nonirradiated and irradiated samples were spotted along with the culture treated with MSN, RB and MSN-RB conjugate. Growth differences were recorded after incubation of plates at 37 °C for 48 h.

Detection of ROS

Endogenous ROS detection was performed with fluorescence spectroscopy using 2′,7′dichlorfluorescein-diacetate (DCFH-DA) [28]. The cells were centrifuged at 10,000 g for 10 min from an overnight culture and the pellet obtained was washed twice with sterile PBS. The pellet after washing was resuspended in PBS and was adjusted to 0.5 McFarland standard followed by incubation for 10 min with 5 μM DCFH-DA reagent. At the end of incubation, the cells were treated with amino functionalized MSN, RB and MSN-RB conjugate and irradiated with 532 nm laser light while the control was left untreated. The fluorescence intensity was measured by exciting at 485 nm.

Cytoplasmic leakage assay

Cytoplasmic leakage of protein from cells was determined according to the protocol mentioned by Singh et al. [7] with little modification. Estimation of protein presence was determined using standard Bradford method [26]. Percentage of protein leaked was calculated in comparison with a positive control. The cells treated with CTAB (N, Cetyl-N,N,N- trimethylammonium bromide) was used as positive control for the assay. Overnight culture was adjusted to 0.5 McFarland standard using sterile PBS and treated with amino functionalised MSN, RB and MSN-RB making a final volume of 1 ml. After 3 h incubation at 37 °C, the samples were irradiated using laser light for 5 min. Similar experiment was performed in dark condition. After irradiation, both light and dark treated cells were centrifuged, and supernatant was collected for the estimation of protein using Bradford method. The Bradford reagent consist the dye Brilliant Blue G in phosphoric acid and methanol or ethanol. Brilliant Blue G forms a complex with proteins in solution resulting in a shift in the absorption maximum of the dye from 465 to 595 nm. The absorption is proportional to the amount of protein present.

DNA damage assay

C. albicans (10^6 CFU/mL) was incubated for 3 h after adding amino functionalized MSN, MSN-RB and RB making to a final volume of 1 ml and irradiated with 532 nm green laser for 5 min. *C. albicans* DNA was extracted immediately after the light treatment using standard procedure. One setup without light treatment was also maintained and DNA extraction was performed. All the isolated DNA samples were analysed using 0.8% agarose gel electrophoresis under Gel DocTMXR + with image lab software (BIO-RAD) [29,30].

Lipid peroxidation assay

The determination of lipid peroxidation in cell membranes of *C. albicans* exposed to green laser after treatment with amino functionalised MSN, RB, MSN-RB was performed using TBARS assay. Cells were irradiated prior to treatment in the same way as in the antimicrobial photodynamic inactivation experiments. About 6% w/v trichloroacetic acid (TCA) was added to treated cell suspensions to precipitate the cell proteins followed by incubation at room temperature for 30 min. Then the samples were centrifuged at 11,000 g for 30 min and to the supernatant 1% aqueous TBA (Sigma-Aldrich, > 98%) solution was added in a ratio of 1:1. The mixture was boiled for 30 minutes, cooled to room temperature overnight and the absorption spectra of the solutions were measured using a UV–Vis spectrometer at 532 nm [31].

Biofilm inhibition assay

Biofilm formation was determined using protocol of Misba et al. [28] with slight modification. The overnight culture was adjusted to 0.5 McFarland standard in YPD broth and was treated and incubated for 3 hours after adding amino functionalised MSN, MSN-RB conjugate and RB (50 µg each) with respective control blanks in 96 well microtitre plates. After incubation, the samples were irradiated using green laser (532 nm wavelength) for 5 min. similar experiments were conducted without irradiation. Both setups were then incubated overnight for about 48 h at 37 °C. The plates were rinsed with sterile PBS after incubation to remove the unadhered cells. Each well was added with 200 µl of 0.1% crystal violet and kept for 15 min and washed with PBS. The cell bound dye was extracted by adding 100 µl of 95% ethanol. Optical density at 595 nm was taken and the absorbance of the blank was subtracted from test values. The percentage of biofilm inhibition was calculated using formula;

$$\textit{Biofilm inhibition}\ (\%) = \frac{\textit{Control } OD_{595nm} - \textit{Test } OD_{595nm}}{\textit{Control } OD_{595nm}} \times 100$$

Cell viability assay

Cell viability assay was performed using TTC (tetrathiozolium chloride) as per the protocol mentioned by Misba et al. [32] with slight modification. The overnight Candida culture was diluted to 0.5 McFarland standard and treated with amino functionalised MSN, RB and MSN-RB conjugate (50 µg each). This was incubated for 3 hours prior to irradiation with laser. Similar experiments were conducted without irradiation. After exposure, 200 µl of fresh broth was added to form biofilm and both non-irradiated and irradiated samples were incubated at 37 °C for 48 h. After incubation the samples were washed twice with sterile PBS to remove unadhered cells. Then 100 µl of 0.5% TTC reagent was added and kept for 30 min and absorbance was measured at 490 nm to determine the formation of formazan indicating the presence of live cells. The percentage reduction of cell viability was calculated accordingly using formula;

$$\textit{Reduction in cell viability}\ (\%) = \frac{\textit{Control } OD_{490nm} - \textit{Test } OD_{490nm}}{\textit{Control } OD_{490nm}} \times 100$$

Influence of aPDT on EPS production

The evaluation of exopolysaccharide (EPS) production was determined using Congo red (CR) binding assay as mentioned by Misba et al. [32]. Overnight growth culture of *C. albicans* was diluted to 10^6 CFU/mL into fresh BHI with 1% glucose which was then treated with amino functionalised MSN, RB and MSN-RB (50 µg/ml each) and irradiated for 5 min after incubation at 37 °C for 3 h. The samples were incubated for 48 h at 37 °C and then the medium was removed, and biofilms were washed with PBS twice. About 100 µl of fresh medium was added to each well including the controls.

To each well of microtitre plate about 50 µL of CR (0.5 mM) was then added and also100 µL of fresh broth along with 50 µL CR was added to another well for blank measurements (Blank CR). Plates were incubated for 2 h and the medium in each well was transferred to 500 µL microcentrifuge tubes and centrifuged at 10,000 rpm for 5 min. The supernatant was transferred to empty wells in microtitre plates and the absorbance was measured at 490 nm. The absorbance value of the supernatant was subtracted from the absorbance value of the 'blank CR'. The percentage reduction in EPS production was calculated using formula;

$$\textit{Redution of EPS production}\ (\%) = \frac{\textit{Control } OD_{490nm} - \textit{Test } OD_{490nm}}{\textit{Control } OD_{490nm}} \times 100$$

Confocal laser scanning microscopy (CLSM)

The effect of *aPDT* on a 48 h grown biofilm of *C. albicans* was analysed using Confocal Laser scanning Microscope as mentioned by Kumari et al. [33]. For CLSM analysis, the biofilm formed on cover slips was treated with amino functionalized MSN (50 µg), MSN-RB nanoconjugate (50 µg) and with free RB (50 µg). Untreated culture was maintained as positive control. After 3 h incubation, all the samples were irradiated using low power green laser with 532 nm wavelength for 5 min [31–33]. Similar experiments were performed in dark. After treatment all the samples were incubated for 48 h at 37 °C. Both irradiated and nonirradiated samples were washed with sterile PBS to remove planktonic cells after incubation. Cells in the biofilm were stained with acridine orange and ethidium bromide dye and were left for 15 min at 37 °C. Fluorescence emission was observed using a LSM 710 (Carl Zeiss Microscopy GMBH, Germany) confocal laser scanning microscope equipped with argon laser with an excitation wavelength of 488 nm.

Statistical analysis

The results were presented as mean ± standard deviation (SD) of individual experiments in triplicate and were compared with those of the control groups. One-way analysis of variance (ANOVA) was used for the comparison with multiple means using turkey test. Data with p-values ≤ 0.05 were considered as statistically significant and recorded and reported.

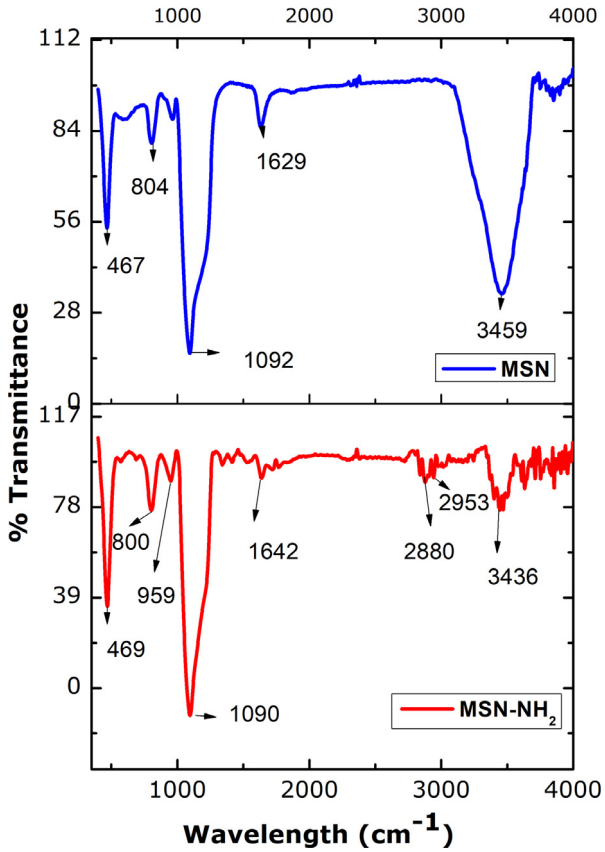

Fig. 1. FTIR spectra of MSN and amino functionalized MSN.

Results and discussion

Characterization of amino functionalised MSN

The surface functionalization of mesoporus nanoparticles with amino groups were confirmed using fourier transform infrared spectroscopy (FTIR). Fig. 1 exhibits the FTIR spectra of MSN and amino functionalized MSN. The strong peaks observed at 804, 964 and 1092 cm^{-1} in MSN and 800, 959, 1090 cm^{-1} in MSN–NH_2 are due to the stretching vibrations of Si-O-Si, Si-OH and Si-O respectively and are the specific peaks of mesoporus silica nanoparticles [44]. The broad peak at 3459 cm^{-1} in MSN was due to O–H vibration. Additional peaks were appeared in amino functionalized MSN at 1642 cm^{-1} is ascribed by the bending vibration of N–H group and 2643 cm^{-1} was due to very strong stretching vibration of C = N. The strong peaks at 2880, 2953 cm^{-1} represented asymmetric and symmetric stretching modes of NH_2 groups [45]. The broad peak at 3436 cm^{-1} is representing stretching vibration of amino group. Amino functionalization of mesoporus silica was confirmed from the peaks observed in FTIR spectra.

Amino functionalization of MSN was performed in order to increase the electrostatic interaction between photosensitizer, since rose bengal is an anionic photosensitizer, a positive charge on MSN will improves this interaction [34]. Functionalization process was performed using 3-Aminopropyltrimethoxysilane (APTMS, 95%) in solvent ethanol [25]. Amino functionalization was confirmed by FTIR analysis and the peak observed in MSN-NH_2 at 1642 cm^{-1} is ascribed by the bending vibration of N–H group and 2643 cm^{-1} was due to very strong stretching vibration of C=N. The strong peaks at 2880, 2953 cm^{-1} represented asymmetric and symmetric stretching modes of NH_2 groups. The peaks were similar in case with other reports for both mesoporus silica and amino functionalized MSN [25,35]

Preparation of amino functionalised MSN- RB conjugate

After conjugation a pink powder was obtained, and it was stored in dark condition. The amino functionalization enhanced the binding of anionic dye rose bengal to its surface. The further characterization studies confirmed the conjugation of RB on to amino functionalized MSN.

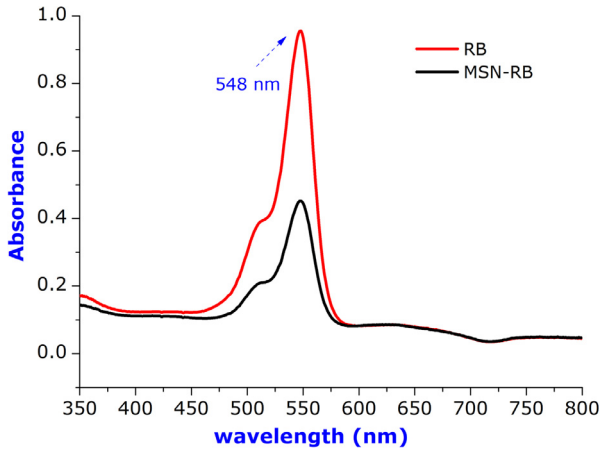

Fig. 2. UV–Vis absorption spectra of RB and MSN-RB conjugate.

Characterization of MSN-RB conjugate

UV–Vis spectroscopic analysis

The UV–Vis spectra obtained for both RB and MSN-RB is depicted in the Fig. 2. The characteristic absorption spectrum for RB was obtained at 540 nm and a similar peak with less absorbance intensity was obtained at 540 nm for MSN-RB nanoconjugate. The similarities in absorption spectrum of RB and MSN-RB confirmed the conjugation process (Fig. 2.) The UV–Vis spectrometric studies about MSN were in agreement with this study [23].

Fourier transform infrared (FTIR) analysis

The FTIR spectra were recorded to confirm the conjugation of RB with mesoporus silica nanoparticles. The FTIR spectra obtained for amino functionalized MSN, RB and MSN-RB is represented in Fig. 3. The strong peaks observed at 800, 959, 1090 cm^{-1} in MSN is due to the stretching vibrations of Si-O-Si, Si-OH and Si-O respectively and 1642, 2843, 2880, 2953 cm^{-1} represents the vibrational peaks of amino groups. In Fig. 3(B), strong C=C stretching vibrations in aromatic ring is observed at 1343, 1455 and 1548 cm^{-1} and O–H stretching vibration was represented by 568 and 3411 cm^{-1}. The carbon skeletal vibrations were observed at 534, 615 and 1611 cm^{-1}. The FTIR spectra of MSN-RB conjugate clearly depicts the presence of both MSN and RB. The similar strong and specific peaks of silica nanoparticles is observed at 801, 953 and 1094 cm^{-1} and the peaks at 1342, 1455 and 1547 cm^{-1} confirms the presence of RB with strong aromatic C=C stretching vibrations. The broad peak at 3632 cm^{-1} was due to N–H or O–H stretching vibration. The FTIR spectra analysis revealed the bands observed for MSN-RB conjugate was in agreement with the peaks individually observed for MSN and RB, thus confirming the conjugation [25,36,37]

Fluorescent spectroscopic analysis

Fluorescent emission spectra (PL spectra) of RB and MSN-RB were recorded at excitation wavelength 540 nm and spectrum obtained is illustrated in Fig. 4(A) and (B). A similar emission peak was obtained for both RB and MSN-RB conjugate at 565 nm. This confirmed the conjugation of RB on MSN. PLE spectrum observed for RB and MSN-RB is illustrated in Fig. 4(C) and (D) and it describes the maximum excitation at 540 nm for both RB and MSN-RB conjugate. So, for both RB and MSN-RB the emission spectra were overlapping at 565 nm. The photoexcitation results observed for RB and MSN-RB at 540 nm was in agreement with UV–Vis absorption peak, confirming the results of conjugation process [23].

HRTEM analysis

HRTEM analysis was performed to determine the shape, size, morphology and dispersity of MSN-RB nanoconjugate. HRTEM analysis of the MSN-RB revealed that the nanoconjugate has monodispersed spherical nanoparticles without any agglomeration. The particles were evenly distributed with an average size of 500 nm (Fig. 5). These spherical and well dispersed nanoparticles enhance the loading and entrapment efficiency of the photosensitizer due to their large surface area along with pores [46].

Dye loading capacity and entrapment efficiency

The dye loading capacity of amino functionalized MSN was found to be $11.44 \pm 0.33\%$. Loading capacity is greatly influenced by the surface functionalization of positively charge amino groups. The anionic dye Rose bengal can easily interact with these with amino groups and can contribute to high loading capacity and entrapment efficiency. The entrapment efficiency of RB was found to be $58.54 \pm 0.75\%$. According to Yan et al. [26], the loading of RB on MSN is only 8% . The MSN-RB

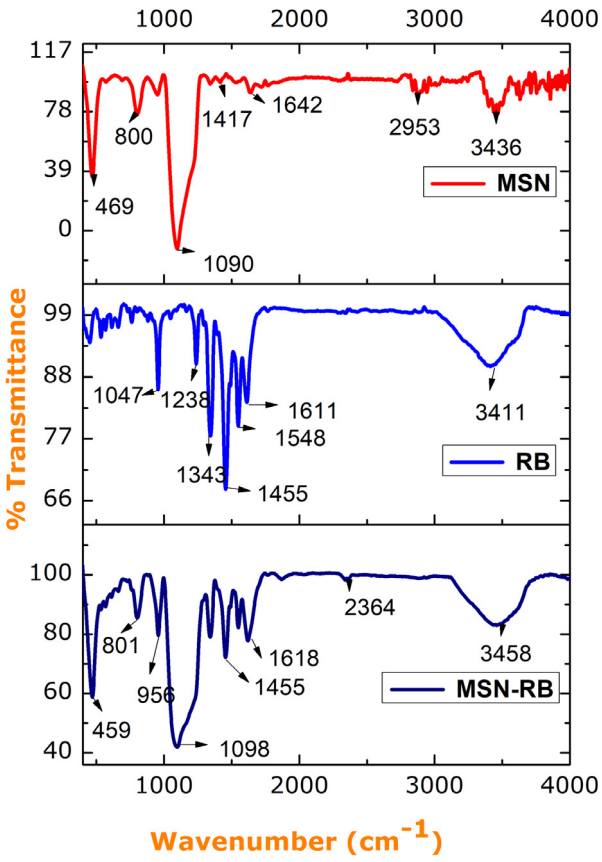

Fig. 3. FTIR spectra of MSN, RB and RB-MSN.

Table 1
Cellular uptake profile of RB and MSN–RB at different intervals of time.

TIME (Hrs)	1	2	3
% UPTAKE RB	33.77 ± 0.47	36.11 ± 0.71	9.33 ± 0.07
% UPTAKE MSN-RB	28.31 ± 0.75	53.03 ± 3.04	46.69 ± 4.2

conjugate in this study showed more loading of RB than mentioned earlier. This confirms that the functionalization with amino groups has improved efficiency to interact with the anionic photosensitizer thus increasing the loading capacity.

In vitro RB release from MSN-RB

The amine groups present in the inner pore surfaces of MSN led to controlled release of the RB molecules by electrostatic attraction is depicted in the Fig. 6. The maximum release of RB was found to be 66.38 ± 5.67% after 3 h. This slow and controlled release of dye is more important for *aPDT* studies. This sustained release in *aPDT* is more advantageous to enhance the excellent activity with less incubation time and facilitate repeated exposure to photodynamic therapy after single administration of MSN-RB conjugate.

Cellular uptake study

The cellular uptake study was performed for both RB and MSN-RB conjugate and the results obtained are represented in the Table 1. The maximum cellular uptake of 53.03 ± 3.04% was observed for MSN-RB after 2 h and was significantly high when compared to free dye. Consequently, the uptake of MSN-RB is more efficient and controlled as the dye is conjugated to a nano platform like mesoporus silica. The cellular uptake of MSN-RB was obtained within 2 h and this also accounts for less incubation time and immediate eradication of microbes through *aPDT*.

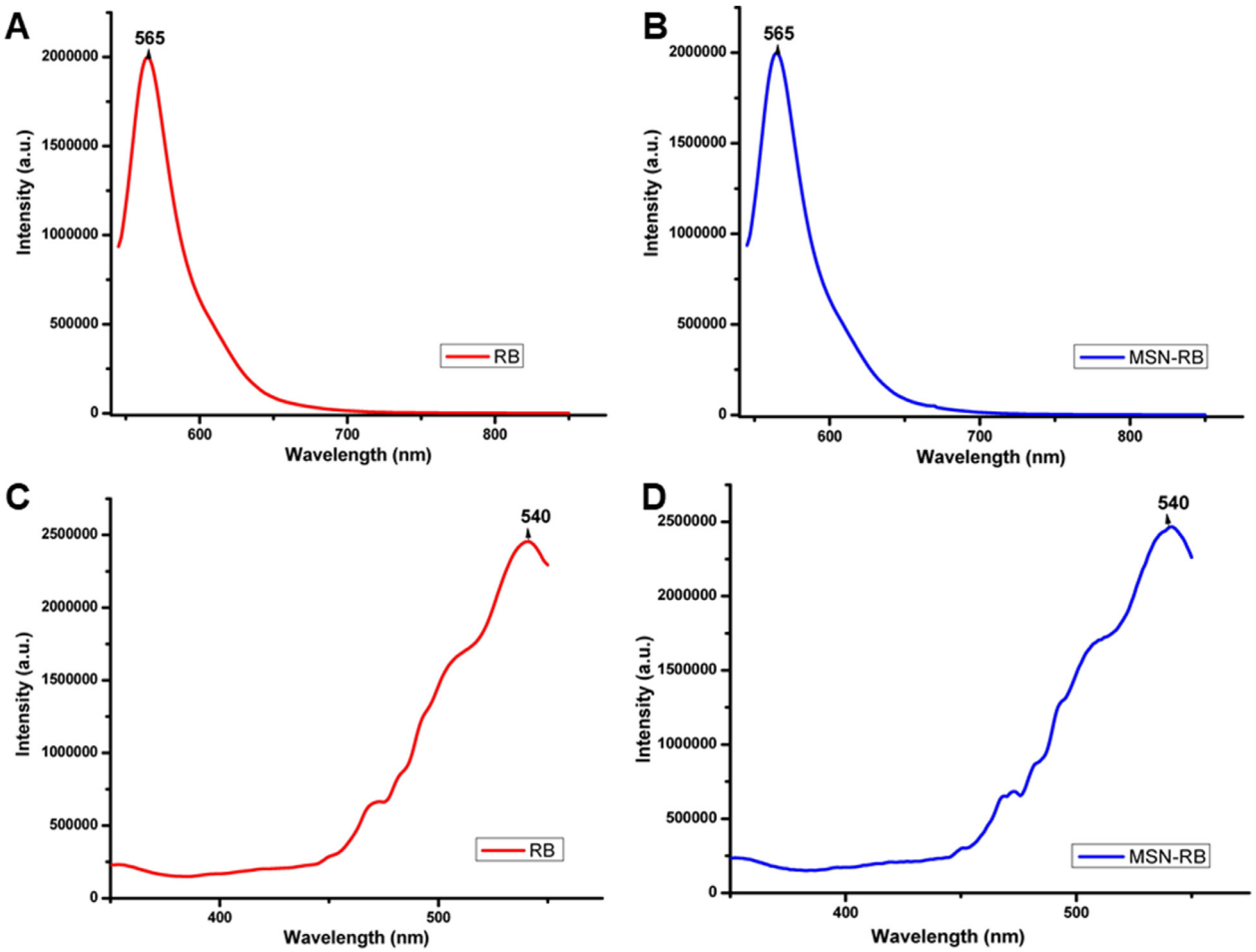

Fig. 4. (A) and (B) Photoemission spectra of RB and MSN-RB conjugate and (C) and (D) excitation spectra of RB and MSN-RB, respectively.

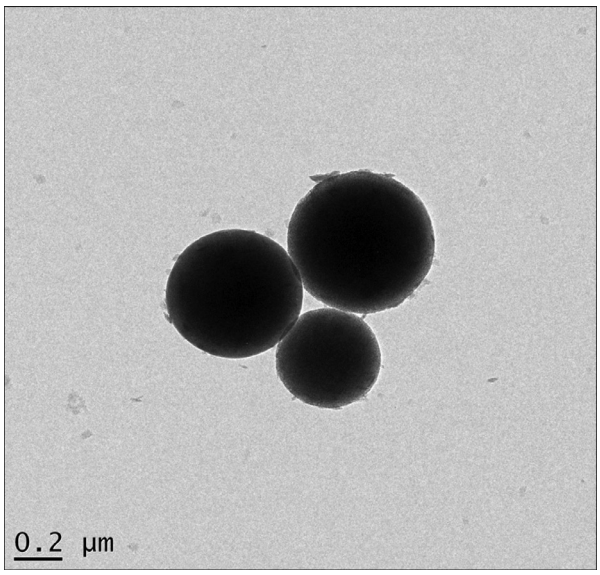

Fig. 5. HRTEM micrograph of MSN-RB nanoconjugate.

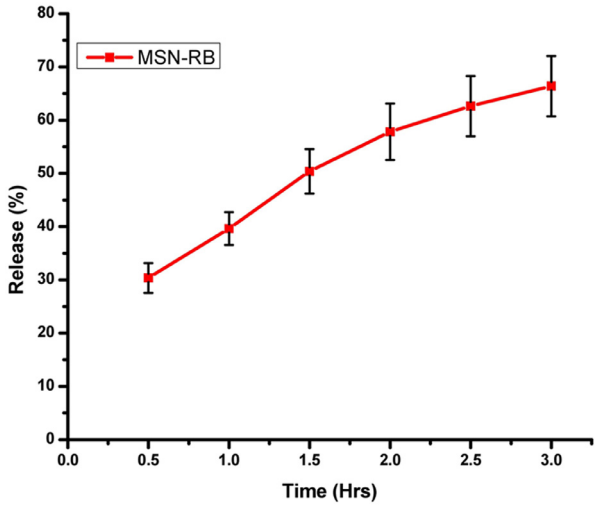

Fig. 6. In vitro release percentage of RB from MSN-RB conjugates. Error bars represent the standard deviation of triplicate experiments.

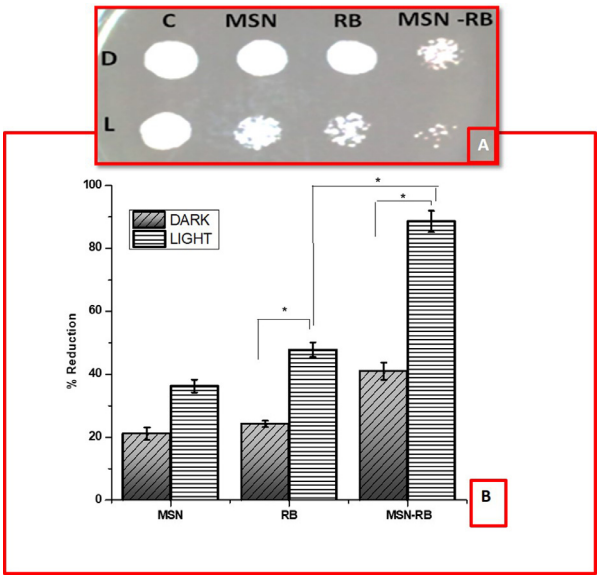

Fig. 7. (A) Spot assay to determine the effect of *aPDT* in both dark and light conditions on *C. albicans*. D and L represent dark and light treated samples respectively. (B) Effect of aPDT on planktonic cells of *C. albicans* after treatment with MSN, RB, MSN-RB. Error bars represent the standard deviation of triplicate experiments. *Represents significance level $p < 0.05$.

Antimicrobial photodynamic inactivation of planktonic cells

The antimicrobial activity of MSN, RB and MSN-RB conjugate with and without irradiation was evaluated using plate count method and the percentage reduction in number of cells were calculated. There was a significant reduction of cells in MSN-RB treated conjugate compared to free dye. About $88.62 \pm 3.4\%$ reduction in cell number was observed for MSN-RB light treated samples while RB treated sample showed only $40.96 \pm 2.71\%$ reduction. The percentage reduction in number of cells is illustrated in Fig. 7(B). In Fig. 7(A) represents the spot assay that further confirms the antimicrobial photodynamic inactivation of cells. Compared to dark treated samples, light treated showed efficient and significant antimicrobial activity [47,48]. Antimicrobial photodynamic inactivation of planktonic cells when irradiated for 5 min resulted in a significant reduction in cell number revealing that MSN-RB conjugate is more efficient than RB alone when compared to the results of Costa et al. [19]. This difference in susceptibility is attributed to the use of nanovehicle (MSN) as it improved the binding, loading and release of RB into the *C. albicans* cells.

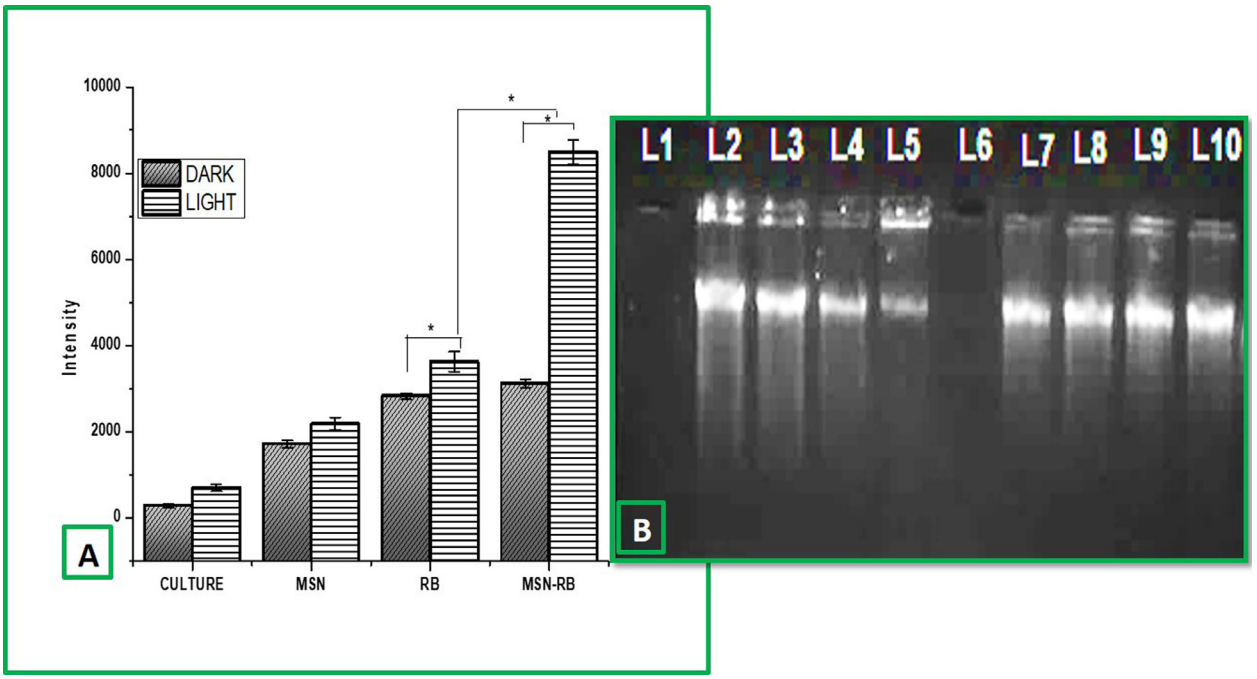

Fig. 8. (A) Total reactive oxygen species detection in *C. albicans* by MSN, RB and MSN-RB evaluated by fluorescence intensity of DCF produced. (B) Agarose gel electrophoresis of chromosomal DNA from *C. albicans* subjected to photodynamic therapy using MSN, RB and MSN-RB respectively. Lane 2–5 are DNA isolated from irradiated samples and Lane 7–10 are DNA isolated from non-irradiated culture. Lane 1 and 6 are blank. Lane 2 and 7 are controls, lane 3 and 8 are MSN treated, lane 4 and 9 are RB treated and lane 5 and 10 are MSN-RB treated samples.

Detection of ROS

A significant increase in DCF fluorescence is observed in MSN-RB treated samples after irradiation compared to control (culture), MSN and RB. The fluorescent intensities obtained for each sample in dark and light treatment is illustrated in the Fig. 8(A). Increase in fluorescence was observed in MSN-RB treated samples compared to the control. The prepared conjugate has more efficiency to produce singlet oxygen and other free radicals compared to MSN and RB [49]. The graph is plotted considering the fluorescent intensities of each sample. The maximum florescence intensity indicate the generation of cellular ROS observed in MSN-RB treated *C. albicans* which substantiate potential antimicrobial efficiency of the newly prepared nanoconjugate [38].

Cytoplasmic leakage

The percentage of protein leakage was calculated and represented in Fig. 9(A). After irradiation, the MSN-RB treated sample released a significantly high amount of protein compared to MSN, and RB. The maximum percentage of protein leakage was found to be $55.18 \pm 3.8\%$ in MSN-RB treated culture. The studies regarding mechanism of action of *aPDT* validated the present study. Cytoplasmic leakage of cellular components justified that membrane is the major site of damage caused by the MSN-RB conjugate which is comparable with the previous studies [26,50].

DNA damage

DNA damage assay resulted in a reduction in the intensity of DNA band due to a reduction in several cells in Fig. 8(B), lane 2–5 represent DNA from irradiated culture and lane 7–10 represent the nonirradiated culture. In lane 5, DNA from the irradiated culture treated with MSN-RB shows less intensity bands. The study also exhibited an apparent decrease in intensity of bands of DNA in the gel [38,39]. This was in agreement with the previous report by Asok et al. [39]. DNA damage assay confirmed that MSN-RB conjugate has internalized into the cells [40].

Lipid peroxidation

Reactive oxygen species (ROS), such as singlet oxygen, produced during the photochemical process of *aPDT* resulted in oxidative damage of lipids present in cells. Lipid peroxidation (MDA product) after *aPDT* experiments was evaluated and the results represented that the lipid peroxidation has occur more in MSN-RB treated culture. Fig. 9(B) depicts the increase

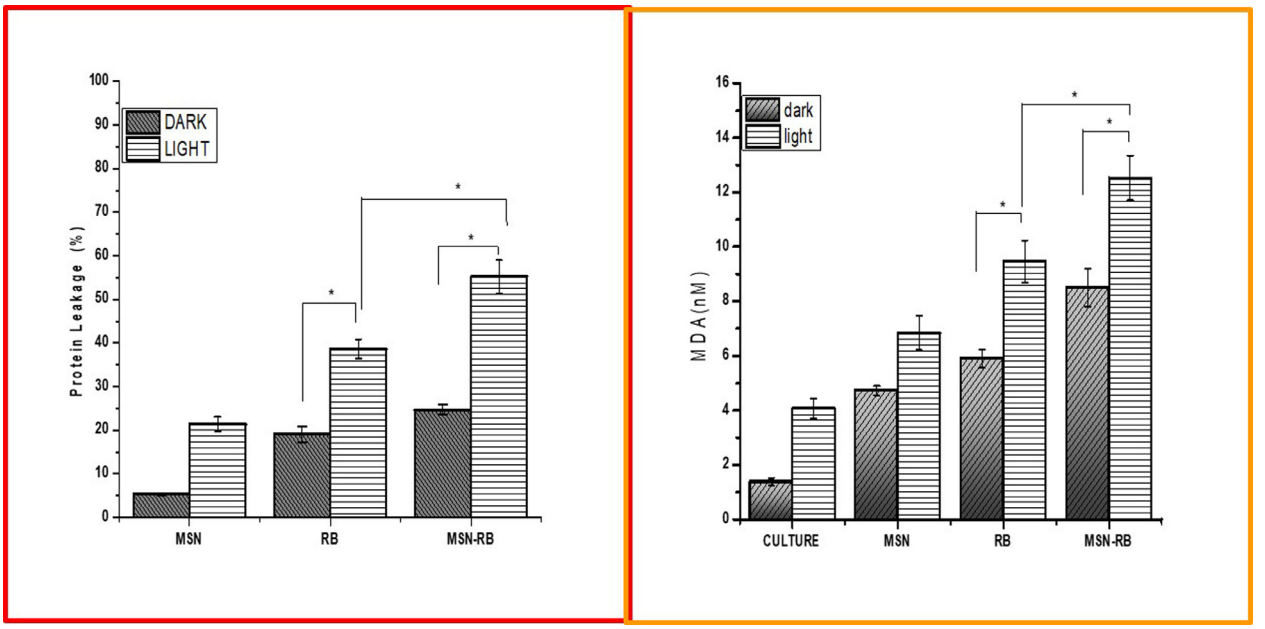

Fig. 9. (A) Percentage Protein leakage after *aPDT* treatment of *C. albicans* with MSN, RB and MSN-RB. Error bars represent the standard deviation of triplicate experiments. *Represents significance at $p < 0.05$. (B) Peroxidation of lipids measured by the formation of malondialdehyde in control (culture), culture treated with MSN, RB and MSN-RB. Error bars represent the standard deviation of triplicate experiments.

in lipid peroxidation with light treated samples measured by the formation of Malondialdehyde (MDA). Lipid peroxidation results were in agreement with the previous study of de Menezes et al. [31].

DNA damage, Protein leakage and lipid peroxidation in *aPDT* has been reported earlier as a cause of cell death in various studies as the ROS mainly target cell membrane, DNA and other biomolecules. This is further confirmed in the present study as the *aPDT* treatment of *C. albicans* with MSN-RB made oxidation of the cell membrane and degradation. The *aPDT* induced photodamage to microbial constituents and resulted in further morphological and functional changes in the microbial cells. The loss of enzyme activities, protein oxidation and formation of protein–protein crosslinks, and inhibition of cellular metabolic processes (e.g., DNA synthesis, glucose transport) and direct damage to the cell membrane leads to leakage of cellular contents following inactivation of the membrane transport system. Since this acts on multiple targets, it is very difficult to a microbe to escape and become resistant to photoinactivation [40].

Biofilm inhibition assay

The antibiofilm activity of MSN, RB and MSN-RB was primarily analysed using the crystal violet binding assay and the percentage inhibition of biofilms was calculated and depicted in Fig. 10(A). Biofilm inhibition was observed more in light treated samples and among that MSN-RB showed a potential and significant antibiofilm activity. The percentage inhibition of biofilm formation by MSN-RB conjugate was calculated to be $79.64 \pm 3.05\%$ whereas RB showed only $42.2 \pm 2.6\%$ at a concentration of 50 µg/ml [18]. These results may be explained by the high chemical reactivity of the photosensitizer which ensures a direct effect on other non-cellular biomolecules and thus inhibits the biofilm formation and virulence of *C. albicans*.

Cell viability assay

The antibiofilm efficacy was further confirmed by checking the cell viability after treatment. The metabolic activity was measured using TTC assay and the percentage reduction in cell viability was calculated and represented in Fig. 10(B). MSN-RB treated culture showed a significant reduction in viable cells compared to RB and MSN after irradiation. The maximum reduction in viable cells was found to be $89 \pm 6.9\%$ for MSN-RB light treated culture. The results of TTC assay performed to evaluate the cell metabolism after irradiation was comparable with the result of Ribeiro et al. [41].

Influence of aPDT on EPS

The production of EPS is an essential part of biofilm formation, for its maturation maintenance. The production of EPS is estimated using Congo red binding assay and the percentage reduction in EPS production was calculated compared to the control culture. The percentage reduction in EPS production is represented in Fig. 10(C). The maximum reduction in

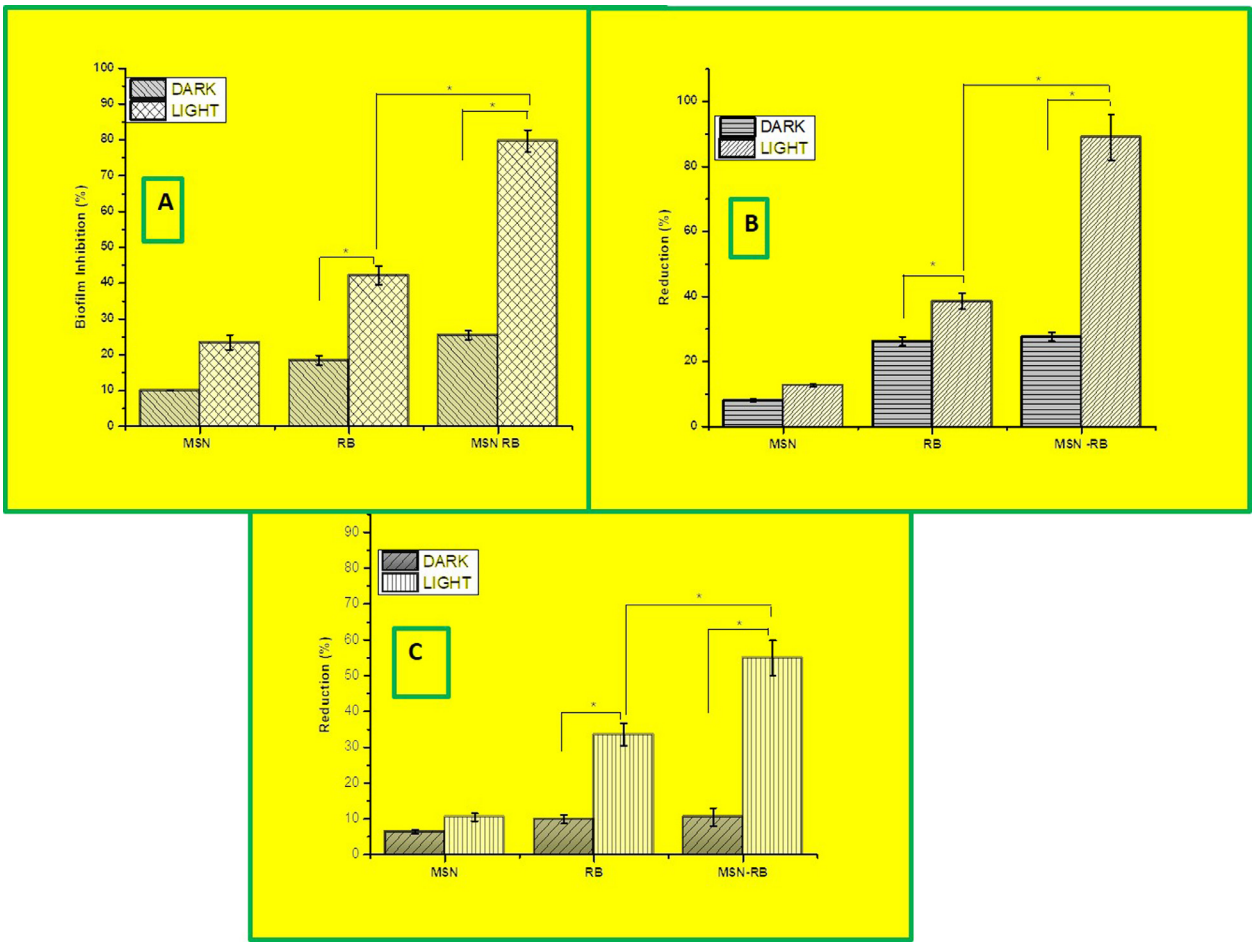

Fig. 10. (A) Crystal violet staining assay to determine the biofilm inhibition in *C. albicans* after *aPDT* treatment with MSN,RB, MSN-RB (B) TTC assay representing the reduction in live cells after *aPDT* treatment with MSN, RB, MSN–RB (C) Congo red binding assay to evaluate the reduction of EPS formed in *C. albicans* upon treatment with MSN, RB and MSN-RB. Error bars represent the standard deviation of triplicate experiments. *Represents significance at $p < 0.05$.

EPS production was observed to be $54.93 \pm 4.9\%$ in MSN-RB treated culture after irradiation. This result reveals a significant reduction in EPS production by the MSN-RB treated cells after 5 min of irradiation.

Confocal laser scanning microscopy (CLSM)

A CLSM study was performed to observe the effect of *aPDT* on the viability and integrity of *C. albicans* biofilm. Mature biofilm after 48 h was incubated with MSN, RB and MSN-RB then irradiated with 532 nm of light. The result observed is illustrated in Fig. 11. In control culture, cells showed green fluorescence indicated that they all were alive. Biofilms treated with MSN, RB and MSN-RB was observed to have both green (live) and red (dead) fluorescence indicated the presence of dead cells throughout biofilm. The maximum red fluorescence was observed in culture treated with MSN-RB conjugate indicating a significant number of dead cells. CLSM analysis confirmed the cell death in biofilm in MSN-RB treatedculture after irradiation.

From the present study, it is revealed that the prepared nanoconjugate (MSN-RB) significantly enhanced antimicrobial photodynamic therapy against planktonic cells as well as biofilm of *C. albicans*. Antimicrobial activity of MSN-RB nanoconjugate is more efficient against *C. albicans* due to higher PS binding efficiency, enhanced ROS production, protein leakage, DNA damage, lipid peroxidation and significant biofilm reduction than that of free dye (Fig. 12). MSN-RB can be used to eradicate the growth and virulence of *C. albicans* significantly. The nanoconjugate of present study could be used to treat localized superficial infections caused by antifungal drug resistant strains and biofilm forming strains such as *C. albicans* that are more difficult to eradicate. Application can also extend to iradicate of these strains on medical devices such as implants and catheters.

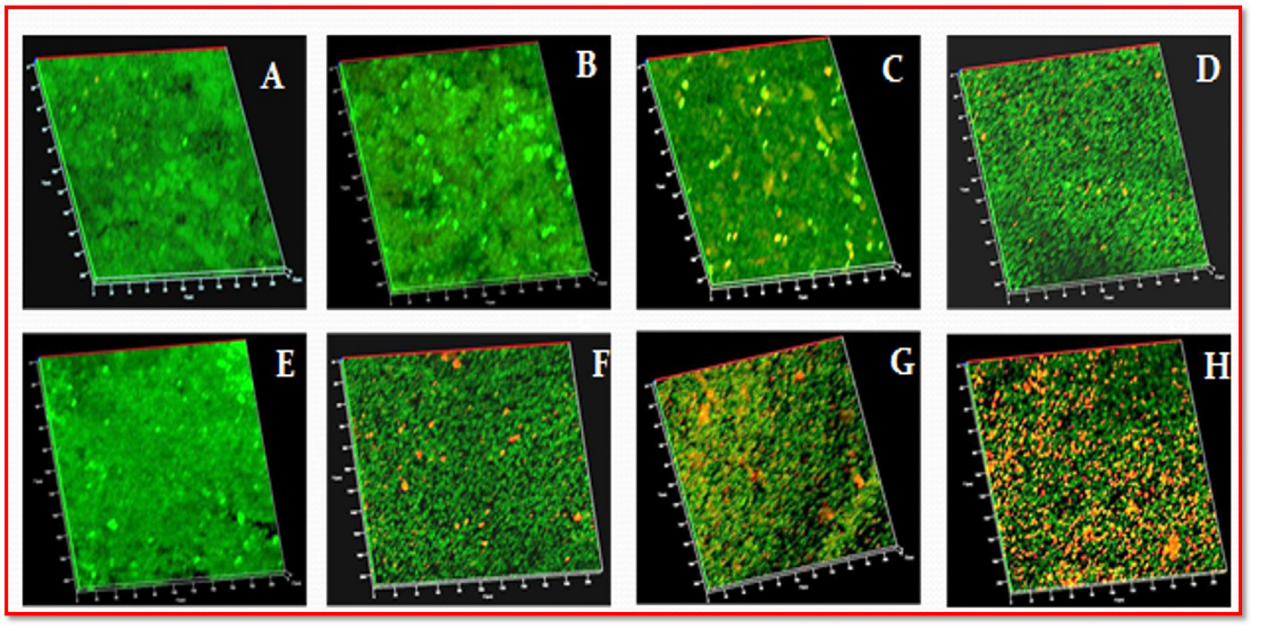

Fig. 11. Live and dead cells in biofilm of *C. albicans* viewed by Confocal laser scanning microscopy. (A) and (E) 3D images of control biofilm in dark and light respectively; (B) and (F) MSN treated cells in dark and light; (C) and (G) RB treated cells and (D) and (H) MSN-RB treated cells in dark and light, respectively.

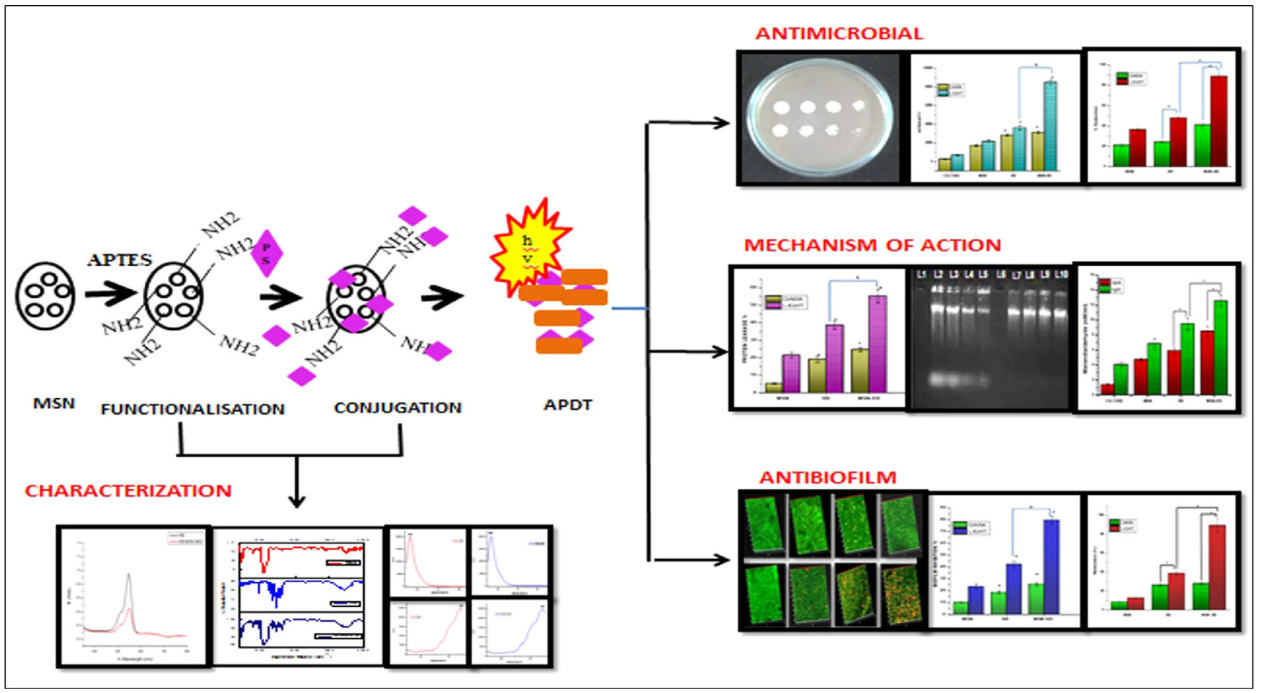

Fig. 12. Schematic representation of synthesis, characterization and antimicrobial activity of MSN-RB conjugate.

Conclusions

The present study highlights the enhanced efficiency of newly synthesized MSN-RB conjugate as an antimicrobial photosensitizer to act against both planktonic and biofilm forms of *Candida albicans*. The enhanced antimicrobial activity of MSN-RB nanoconjugate is more efficient against *C. albicans* due to high PS binding efficiency, enhanced ROS production, protein leakage, DNA damage, lipid peroxidation and significant biofilm reduction than that of free dye. Fluorescent spectroscopic

analysis validated the generation of ROS and cytoplasmic leakage and lipid peroxidation assay confirmed the membrane damage that facilitated the leakage of protein and other components out of the cell. To the best of our knowledge, this is the first report. Amino functionalized mesoporus silica conjugated rose Bengal (MSN-RB) was used as an antimicrobial photosensitizer to enhance the effect of antimicrobial photodynamic therapy against *C. albicans*. From this study, it can be concluded that the prepared MSN-RB conjugate can eradicate the growth and virulence of *C. albicans* significantly. This can be used to treat localized superficial infections caused by antifungal drug resistant and biofilm forming strains. Application can also extend to iradicate these strains on medical devices such as implants and catheters.

Acknowledgement

We are grateful to the Department of Physics, Pondicherry University for providing the facility of laser treatment and Central Instrumentation Facility, Bharathidasan University, Tiruchirappalli, India, for the CLSM analysis. We are thankful to iThemba LABS-National Research Foundation (NRF), Somerset West, South Africa for the HRTEM facility.

Conflict of interest

There are no conflicts of interest to declare.

References

[1] F. Pereira Gonzales, T. Maisch, Photodynamic inactivation for controlling *Candida albicans*infections, Fungal Biol 116 (2012) 1.
[2] N. Liu, J. Tu, G. Dong, Y. Wang, C. Sheng, Emerging New Targets for the Treatment of Resistant Fungal Infections, J. Med. Chem. (2018) acs. jmedchem.7b01413.
[3] L.J. Douglas, *Candida* biofilms and their role in infection, Trends Microbiol 11 (2003) 30.
[4] A.P. Pinto, I.B. Rosseti, M.L. Carvalho, B.G.M. da Silva, C. Alberto-Silva, M.S. Costa, Photodynamic Antimicrobial Chemotherapy (PACT), using Toluidine blue O inhibits the viability of biofilm produced by *Candida albicans* at different stages of development, Photodiagnosis Photodyn. Ther. 21 (2018) 182.
[5] T. Jain, P.R. Muktapuram, K. Sharma, O. Ravi, G. Pant, K. Mitra, S.R. Bathula, D. Banerjee, Biofilm inhibition and anti-*Candida* activity of a cationic lipo-benzamide molecule with twin-nonyl chain, Bioorg. Med. Chem. Lett. (2018).
[6] C.G. Pierce, A. Srinivasan, A.K. Ramasubramanian, J.L. López-Ribot, From Biology to Drug Development: New Approaches to Combat the Threat of Fungal Biofilms, in: Microbial Biofilms, 2nd Edition, American Society of Microbiology, 2016, pp. 373–388.
[7] S. Basak, P. Singh, M. Rajurkar, Multidrug Resistant and Extensively Drug Resistant Bacteria: A Study, J. Pathog. 2016 (1) (2016).
[8] A. Penesyan, M. Gillings, I. Paulsen, Antibiotic Discovery: Combatting Bacterial Resistance in Cells and in Biofilm Communities, Molecules 20 (2015) 5286.
[9] N. Høiby, T. Bjarnsholt, M. Givskov, S. Molin, O. Ciofu, Antibiotic resistance of bacterial biofilms, Int. J. Antimicrob. Agents 35 (2010) 322.
[10] L. Yang, Y. Liu, H. Wu, Z. Song, N. Høiby, S. Molin, M. Givskov, Combating biofilms, FEMS Immunol. Med. Microbiol. 65 (2012) 146.
[11] C.-M. Hsieh, Y.-H. Huang, C.-P. Chen, B.-C. Hsieh, T. Tsai, 5-Aminolevulinic acid induced photodynamic inactivation on *Staphylococcus aureus* and *Pseudomonas aeruginosa*, J. Food Drug Anal. 22 (2014) 350.
[12] L. Huang, T.G. St. Denis, Y. Xuan, Y.-Y. Huang, M. Tanaka, A. Zadlo, T. Sarna, M.R. Hamblin, Free Radic. Biol. Med. 53 (2012) 2062.
[13] F. Cieplik, L. Tabenski, W. Buchalla, T. Maisch, Paradoxical potentiation of methylene blue-mediated antimicrobial photodynamic inactivation by sodium azide: Role of ambient oxygen and azide radicals, Front. Microbiol. 5 (2014) 1.
[14] F. Cieplik, A. Späth, J. Regensburger, A. Gollmer, L. Tabenski, K.-A. Hiller, W. Bäumler, T. Maisch, G. Schmalz, Photodynamic biofilm inactivation by SAPYR—An exclusive singlet oxygen photosensitizer, Free Radic. Biol. Med. 65 (2013) 477.
[15] M.R. Hamblin, Antimicrobial photodynamic inactivation: a bright new technique to kill resistant microbes, Curr. Opin. Microbiol. 33 (2016) 67.
[16] G. Jori, C. Fabris, M. Soncin, S. Ferro, O. Coppellotti, D. Dei, L. Fantetti, G. Chiti, G. Roncucci, Lasers Surg. Med. 38 (2006) 468.
[17] Y. Guo, S. Rogelj, P. Zhang, Photodynamic therapy in the treatment of microbial infections: Basic principles and perspective applications, Nanotechnology 21 (2010) 065102.
[18] R.D. Rossoni, J.C. Junqueira, E.L.S. Santos, A.C.B. Costa, A.O.C. Jorge, Comparison of the efficacy of Rose Bengal and erythrosin in photodynamic therapy against Enterobacteriaceae, Lasers Med. Sci. 25 (2010) 581.
[19] A.C.B.P. Costa, V.M.C. Rasteiro, C.A. Pereira, R.D. Rossoni, J.C. Junqueira, A.O.C. Jorge, The effects of rose bengal- and erythrosine-mediated photodynamic therapy on *Candida albican*, Mycoses 55 (2012) 56.
[20] A. Mehmood, H. Ghafar, S. Yaqoob, U.F. Gohar, B. Ahmad, Mesoporous Silica Nanoparticles: A Review, J. Dev. Drugs (2017) 06.
[21] F. Tang, L. Li, D. Chen, Mesoporous Silica Nanoparticles: Synthesis, Biocompatibility and Drug Delivery, Adv. Mater. 24 (2012) 1504.
[22] O. Planas, R. Bresolí-obach, J. Nos, T. Gallavardin, R. Ruiz-gonzález, S. Nonell, Synthesis, Photophysical Characterization, and Photoinduced Antibacterial Activity of Methylene Blue-loaded Amino- and Mannose-Targeted Mesoporous Silica Nanoparticles, Molecules 20 (2015) 6284.
[23] Y. Liu, X. Liu, Y. Xiao, F. Chen, F. Xiao, A multifunctional nanoplatform based on mesoporous silica nanoparticles for imaging-guided chemo/photodynamic synergetic therapy, RSC Adv 7 (2017) 31133.
[24] L. Wasserstrom, D. Portugal-Nunes, H. Almqvist, A.G. Sandström, G. Lidén, M.F. Gorwa-Grauslund, Exploring d-xylose oxidation in *Saccharomyces cerevisiae* through the Weimberg pathway, AMB Express 8 (2018) 33.
[25] P. Khosraviyan, M. Shafiee Ardestani, M. Khoobi, S.N. Ostad, F.A. Dorkoosh, H. Akbari Javar, M. Amanlou, Mesoporous silica nanoparticles functionalized with folic acid/methionine for active targeted delivery of docetaxel, Onco. Targets. Ther. Volume 9 (2016) 7315.
[26] T. Yan, J. Cheng, Z. Liu, F. Cheng, X. Wei, J. He, pH-Sensitive mesoporous silica nanoparticles for chemo-photodynamic combination therapy, Colloids Surfaces B Biointerfaces 161 (2018) 442.
[27] M. Usacheva, B. Layek, S.S. Rahman Nirzhor, S. Prabha, Nanoparticle-Mediated Photodynamic Therapy for Mixed Biofilms, J. Nanomater. 2016 (2016) 1.
[28] L. Misba, S. Kulshrestha, A.U. Khan, Antibiofilm action of a toluidine blue O-silver nanoparticle conjugate on *Streptococcus mutans*: a mechanism of type I photodynamic therapy, Biofouling 32 (2016) 313.
[29] M. SINGH, A.K. Mallick, M. BANERJEE, R. KUMAR, Loss of outer membrane integrity in Gram-negative bacteria by silver nanoparticles loaded with *Camellia sinensis* leaf phytochemicals: plausible mechanism of bacterial cell disintegration, Bull. Mater. Sci. 39 (2016) 1871.
[30] P. Piper, The Pdr12 ABC transporter is required for the development of weak organic acid resistance in yeast, Rapid Isolation of Yeast DNA 15 (1998) EMBO press.
[31] H.D. de Menezes, L. Tonani, L. Bachmann, M. Wainwright, G. Ú., L. Braga, M.R. von Zeska Kress, Photodynamic treatment with phenothiazinium photosensitizers kills both ungerminated and germinated microconidia of the pathogenic fungi *Fusarium oxysporum*, *Fusarium moniliforme* and *Fusarium solani*, J. Photochem. Photobiol. B Biol. 164 (2016) 1.
[32] L. Misba, S. Zaidi, A.U. Khan, A comparison of antibacterial and antibiofilm efficacy of phenothiazinium dyes between Gram positive and Gram negative bacterial biofilm, Photodiagnosis Photodyn. Ther. 18 (2017) 24.

[32] P. Kumari, R. Mishra, N. Arora, A. Chatrath, R. Gangwar, P. Roy, R. Prasad, Nanotechnology in Sustainable Agriculture: Recent Developments, Challenges, and Perspectives, Front. Microbiol. 8 (2017) 1.
[34] I.I. Slowing, B.G. Trewyn, S. Giri, V.S.-Y. Lin, Mesoporous Silica Nanoparticles for Drug Delivery and Biosensing Applications, Adv. Funct. Mater. 17 (2007) 1225.
[35] K. Nakanishi, M. Tomita, K. Kato, Synthesis of amino-functionalized mesoporous silica sheets and their application for metal ion capture, J. Asian Ceram. Soc. 3 (2015) 70.
[36] M. Dabrzalska, N. Benseny-Cases, R. Barnadas-Rodríguez, S. Mignani, M. Zablocka, J.-P. Majoral, M. Bryszewska, B. Klajnert-Maculewicz, J. Cladera, Fourier transform infrared spectroscopy (FTIR) characterization of the interaction of anti-cancer photosensitizers with dendrimers, Anal. Bioanal. Chem. 408 (2016) 535.
[37] A. Popat, J. Liu, G.Q (Max) Lu, S.Z. Qiao, A pH-responsive drug delivery system based on chitosan coated mesoporous silica nanoparticles, J. Mater. Chem. 22 (2012) 11173.
[38] S. Dwivedi, R. Wahab, F. Khan, Y.K. Mishra, J. Musarrat, A.A. Al-Khedhairy, Reactive Oxygen Species Mediated Bacterial Biofilm Inhibition via Zinc Oxide Nanoparticles and Their Statistical Determination, PLoS One 9 (2014) e111289.
[39] A. Asok, E. Arshad, C. Jasmin, S. Somnath Pai, I.S. Bright Singh, A. Mohandas, A. Anas, Reducing: a promising strategy to reduce antibiotic application in shrimp larviculture*Vibrio*: a promising strategy to reduce antibiotic application in shrimp larviculture load in: a promising strategy to reduce antibiotic application in shrimp larviculture*Artemia*: a promising strategy to reduce antibiotic application in shrimp larviculture nauplii using antimicrobial photodynamic therapy: a promising strategy to reduce antibiotic application in shrimp larviculture, Microb. Biotechnol. 5 (2012) 59.
[40] N. Kashef, M.R. Hamblin, Can microbial cells develop resistance to oxidative stress in antimicrobial photodynamic inactivation? Drug Resist. Updat. 31 (2017) 31.
[41] A.P.D. Ribeiro, M.C. Andrade, J. de Fátima da Silva, J.H. Jorge, F.L. Primo, A.C. Tedesco, A.C. Pavarina, Photodynamic Inactivation of Planktonic Cultures and Biofilms of *Candida albicans* Mediated by Aluminum-Chloride-Phthalocyanine Entrapped in Nanoemulsions, Photochem. Photobiol. 89 (2013) 111.
[42] A. Raja, S. Ashokkumar, R. Pavithra Marthandam, J. Jayachandiran, C. Prasad Khatiwada, K. Kaviyarasu, R. Ganapathi Raman, M. Swaminathan, Eco-friendly preparation of zinc oxide nanoparticles using *Tabernaemontana divaricata* and its photocatalytic and antimicrobial activity, J.Photochem. Photobiol. B: Biol. 181 (2018) 53–58.
[43] K. Kanimozhi, S.K. Basha, V.S. Kumari, K. Kaviyarasu, M. Maaza, In vitro cytocompatibility of chitosan/PVA/methylcellulose – Nanocellulose nanocomposites scaffolds using L929 fibroblast cells, Appl. Surf. Sci. 449 (2018) 574–583.
[44] C. Jayakumar, C. Maria Magdalane, K. Kaviyarasu, M. Anbu Kulandainathan, B. Jeyaraj, M. Maaza, Direct Electrodeposition of Gold Nanoparticles on Glassy Carbon Electrode for Selective Determination Catechol in the Presence of Hydroquinone, J. Nanosci. Nanotechnol. 18 (7) (2018) 4544–4550.
[45] K. Kanimozhi, S.K. Basha, V.S. Kumari, K. Kaviyarasu, Development of Biomimetic Hybrid Porous Scaffold of Chitosan/Polyvinyl Alcohol/Carboxymethyl Cellulose by Freeze-Dried and Salt Leached Technique, J. Nanosci. Nanotechnol. 18 (7) (2018) 4916–4922.
[46] C. Maria Magdalane, K. Kaviyarasu, A. Raja, M.V. Arularasu, G.T. Mola, A.B. Isaev, NaifAbdullah Al-Dhabi, MariadhasValan Arasu, B. Jeyaraj, J. Kennedy, M. Maaza, Photocatalytic decomposition effect of erbium doped cerium oxide nanostructures driven by visible light irradiation: Investigation of cytotoxicity, antibacterial growth inhibition using catalyst, J. Photochem. Photobiol. B: Biol. 185 (2018) 275–282.
[47] A. Mobeen Amanulla, S.K. Jasmine Shahina, R. Sundaram, C. Maria Magdalane, K. Kaviyarasu, D. Letsholathebe, S.B. Mohamed, J. Kennedy, M. Maaza, Antibacterial, magnetic, optical and humidity sensor studies of β-$CoMoO_4$ - Co_3O_4 nanocomposites and its synthesis and characterization, J. Photochem. Photobiol. B: Biol. 183 (2018) 233–241.
[48] D. Saravanakkumar, S. Sivaranjani, K. Kaviyarasu, A. Ayeshamariam, B. Ravikumar, S. Pandiarajan, C. Veeralakshmi, M. Jayachandran, M. Maaza, Synthesis and characterization of ZnO–CuO nanocomposites powder by modified perfume spray pyrolysis method and its antimicrobial investigation, J. Semicond. 39 (3) (2018) 033001.
[49] K. Kaviyarasu, K. Kanimozhi, N. Matinise, C. Maria Magdalane, G.T. Mola, J. Kennedy, M. Maaza, Antiproliferative effects on human lung cell lines A549 activity of cadmium selenide nanoparticles extracted from cytotoxic effects: Investigation of bio-electronic application, Mater. Sci. Eng. C 76 (2017) 1012–1025.
[50] K. Kaviyarasu, N. Geetha, K. Kanimozhi, C. Maria Magdalane, S. Sivaranjani, A. Ayeshamariam, J. Kennedy, M. Maaza, In vitro cytotoxicity effect and antibacterial performance of human lung epithelial cells A549 activity of Zinc oxide doped TiO_2 nanocrystals: Investigation of bio-medical application by chemical method, Mater. Sci. Eng. C 74 (2017) 325–333.